

Resonant synchronization and information retrieve from memorized Kuramoto network

Lin Zhang,* Xv Li, and Tingting Xue

School of Physics and Information Technology, Shaanxi Normal University, Xi'an 710061, P. R. China

(Dated: September 6, 2018)

A new collective behavior of resonant synchronization is discovered and the ability to retrieve information from brain memory is proposed based on this mechanism. We use modified Kuramoto phase oscillator to simulate the dynamics of a single neuron in self-oscillation state, and investigate the collective responses of a neural network, which is composed of N globally coupled Kuramoto oscillators, to the external stimulus signals in a critical state just below the synchronization threshold of Kuramoto model. The input signals at different driving frequencies, which are used to denote different neural stimuli, can drive the coupled oscillators into different synchronized groups locked to the same effective frequencies and recover synchronized patterns emerged from their collective dynamics closely related to the predetermined frequency distributions of the oscillators (memory). This model is used to explain how brain stores and retrieves information from the synchronization patterns emerging in the neural network stimulated by the external inputs.

PACS numbers:

I. INTRODUCTION

The consciousness of the human brain and its memory mechanism are the most fascinating problems in physics and biology [1–3]. With the help of molecular biology and the brain magnetic resonance imaging (MRI), neurobiologists have identified the detailed physical structures and the local functions of the brain [4]. Regions of the brain have been proved to be a complex network of well-connected neurons working in a critical state that can exhibit complicated synchronization behaviors during the brain's continuous discharge induced by neutral stimulus from our sensory organs [5]. As synchronized patterns of neurons are indicated to demonstrate the cognitive activities in human brain, many mathematical models have been proposed to study consciousness activities in human brain [6]. However, due to the complexity of the neural network, analytical analysis cannot be carried out efficiently on these models and most numerical works are limited to give apparent behaviors of cognitive activity [7]. Based on the synchronized spatiotemporal patterns emerged in brain activities [8], we adopt Kuramoto model [9, 10], a very simple model of globally coupled nonlinear rotators, to study the collective dynamics of neurons working in a state of self-sustained oscillation and explore their collective behaviors by resonant synchronization phenomenon. Our study shows that Kuramoto model presents a synchronized resonant behavior and which can be used to study presentation or extraction of information from human brain by external stimulation [11–15]. By studying the collective resonance of Kuramoto model, we find that when the coupling strength between Kuramoto oscillators (KOs) is just below the synchronization threshold, the coupled KOs will exhibit an obvious

resonant synchronization when the system is subjected to a resonant external stimulus, and it can exactly provide an explanation of the brain memory to store and retrieve information in its critical neural networks.

II. THE RESONANT SYNCHRONIZATION

A. The synchronized dynamics between two coupled harmonic oscillators by external driving

In order to give a basic idea of the resonant synchronization, we begin with a well-studied model: two coupled linear harmonic oscillators (HOs). First, resonance is a very common dynamic phenomenon in physics, in which a vibrating system or an external force drives another system to oscillate with an increased energy at certain frequencies [16]. Mechanical resonance can accumulate energy to break glass cups or even damage bridges and buildings [17–21]. The dynamical equation to describe resonance is

$$\ddot{x} + 2\gamma\dot{x} + \omega_0^2 x = F_0 \cos \Omega t, \quad (1)$$

where x describes the vibration displacement, ω_0 is the eigenfrequency of the oscillator, γ is the damping rate, F_0 and Ω are the driving strength and frequency, respectively. The motion of the driven oscillator in frequency domain reads

$$x(\omega) = \chi(\omega) F(\omega), \quad (2)$$

where $\chi(\omega)$ is a complex responsive function

$$\chi(\omega) = \frac{1}{(\omega_0^2 - \omega^2) - i(2\gamma\omega)}, \quad (3)$$

which is also called displacement susceptibility. Then the solution of Eq.(1) is an inverse Fourier transformation of

*Email address: zhanglincn@snnu.edu.cn

Eq.(2) by

$$x(t) = |\chi(\Omega)| F_0 \cos(\Omega t - \theta), \quad (4)$$

where $\theta = \arg \chi(\Omega)$ is the phase of $\chi(\Omega)$. Obviously, after a transient dynamics, the frequency of the driven oscillator is locked to driving frequency Ω and its vibration amplitude (energy) reaches maximum when $\Omega \rightarrow \omega_R = \sqrt{\omega_0^2 - 2\gamma^2}$, which is the so called resonant phenomenon. For a high- Q oscillator $\gamma \rightarrow 0$, an obvious dynamical transition between in-phase and out-of-phase motions demonstrates an important synchronized behavior at driving point of $\omega_R \approx \omega_0$. This behavior, especially happens among an ensemble of coupled nonlinear oscillators in a complicated networks, is called resonant synchronization: synchronization induced by resonant driving. In order to illustrate this, we return to two coupled HOs in a configuration of Fig.1(a) (top inset) which are described by

$$\ddot{x}_1(t) + 2\gamma_1 \dot{x}_1(t) + \omega_{01}^2 x_1(t) = K_1 x_2(t) + F(t), \quad (5)$$

$$\ddot{x}_2(t) + 2\gamma_2 \dot{x}_2(t) + \omega_{02}^2 x_2(t) = K_2 x_1(t), \quad (6)$$

where

$$\omega_{01} = \sqrt{\frac{k_1 + K}{m_1}}, K_1 = \frac{K}{m_1}, \quad (7)$$

$$\omega_{02} = \sqrt{\frac{k_2 + K}{m_2}}, K_2 = \frac{K}{m_2}, \quad (8)$$

with k_1 , k_2 and K being the stiffness coefficients of the springs labeled in Fig.1(a). Then the displacement responses of two coupled HOs are

$$x_1(\omega) = \chi_1(\omega) F(\omega), \quad (9)$$

$$x_2(\omega) = \chi_2(\omega) F(\omega), \quad (10)$$

where the displacement susceptibilities are

$$\chi_1(\omega) = \frac{(\omega_{02}^2 - \omega^2) - i2\gamma_2\omega}{(\omega_{01}^2 - \omega^2 - i2\gamma_1\omega)(\omega_{02}^2 - \omega^2 - i2\gamma_2\omega) - k_1 k_2},$$

$$\chi_2(\omega) = \frac{k_2}{(\omega_{01}^2 - \omega^2 - i2\gamma_1\omega)(\omega_{02}^2 - \omega^2 - i2\gamma_2\omega) - k_1 k_2}.$$

Fig.1(a) shows that the amplitude responses of $|\chi_{1,2}(\Omega)|$ to force $F(t) = F_0 \cos \Omega t$ exerted on the first oscillator exhibits two types of resonant peak. The synchronized properties at two resonant frequencies around $\Omega = \omega_{R1}$ and $\Omega = \omega_{R2}$ are shown in Fig.1(b) by the relative phase between two HOs

$$\delta\theta = \arg(\chi_1) - \arg(\chi_2). \quad (11)$$

We can see that when the driving frequency comes near to the resonant frequencies ω_R , the relative phase tends to be connected due to the resonant effect, such as the lower resonant driving frequency ω_{R1} leading to an in-phase vibration (left top inset of Fig.1(b)), and the higher resonant frequency ω_{R2} leading to a $\pi/2$ -lagged vibration

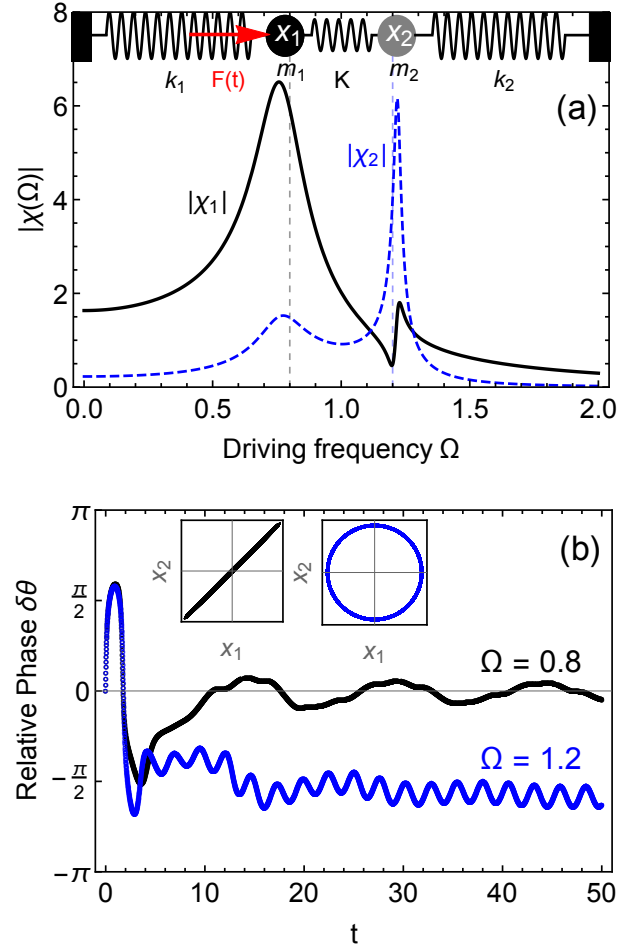


FIG. 1: (color online). (a) The amplitude responsive spectra of two coupled HOs driven by the external force on the first oscillator labeled by x_1 . The vertical dashed lines indicate the driving frequencies of $\Omega = \omega_{R1} \approx 0.8$ and $\Omega = \omega_{R2} \approx 1.2$. Top inset: the configuration of the two coupled HOs driven by force $F(t)$. (b) The relative phase of two HOs driven by resonant frequencies of $\Omega = \omega_{R1}$ and $\Omega = \omega_{R2}$, respectively. Top inset: the longtime related orbits between $x_1(t)$ and $x_2(t)$ at driving frequencies of $\Omega = 0.8$ (left) and $\Omega = 1.2$ (right), respectively. The other parameters are $\gamma_1 = 0.1, \gamma_2 = 0.01$ and $K_1 = K_2 = 0.2$.

(right top inset of Fig.1(b)). This toy model demonstrates that the resonant driving can give manifest influences on the collective amplitude and phase of coupled oscillators, which will lay down the main idea of resonant synchronization for information store and retrieve from the network.

B. Resonant synchronization in Kuramoto model

Basically, synchronization is the correlated dynamical behaviors between coupled nonlinear oscillators, but, for linear HOs, the above correlated dynamics shown in Fig.1

is not strictly synchronization [22]. In 1673, Huygens observed synchronized motion of two adjacent pendulum clocks and opened the study of synchronization, and then various synchronizations are found to reveal a universal phenomenon in nature. For nonlinear oscillators, synchronization is related to the self-sustained (limit-cycle) oscillation, which is a special state that has stable amplitude and free phase [23]. Roughly, there are two important types of synchronization, one is the driven synchronization induced by a stable driving, and the other is the mutual synchronization due to the mutual couplings between oscillators. What we study here is the driven type whose behaviors are closely dependent on the coupling strength and the driving detuning [22]. In recent years, the synchronized behaviors of neurons have received widespread attentions in the study of vision [24], movement [25], memory [26], epilepsy [27–33] and so on.

The Kuramoto model is a typical physical model to exhibit synchronization when the coupling rate k reaches a critical value k_c . In a system with only two coupled KOs, the nonlinear equations of the system are

$$\dot{\theta}_1 = \omega_1 + \frac{k}{2} \sin(\theta_2 - \theta_1), \quad (12)$$

$$\dot{\theta}_2 = \omega_2 + \frac{k}{2} \sin(\theta_1 - \theta_2), \quad (13)$$

where each oscillator has its own eigenfrequency ω_1 or ω_2 , and k is their coupling rate. The system can describe two neurons in limit-cycle states with their pulsing phases θ_i . There are two ways to synchronize KOs: increasing coupling strength k and introducing external driving. In this paper, the driving is introduced to simulate the imagination or thinking process triggered by the neural signals from our sensory organs. Then the full equations are [34]

$$\dot{\theta}_1 = \omega_1 + \frac{k}{2} \sin(\theta_2 - \theta_1) + \Lambda \sin(\Omega t - \theta_1), \quad (14)$$

$$\dot{\theta}_2 = \omega_2 + \frac{k}{2} \sin(\theta_1 - \theta_2), \quad (15)$$

where Λ and Ω are the stimulating strength and frequency, respectively. Keeping the coupling rate k below the synchronization threshold k_c , that is, the system is initially in a non-synchronous state, the KOs synchronize after a transient state by adding an external signal with a frequency close to the eigenfrequencies of the KOs. Fig.2(a) shows the resonant synchronization through Pearson correlation coefficient C_{12} , a dynamical measure to estimate the degree of synchronization between oscillators 1 and 2. When two KOs are completely synchronized or anti-synchronized, the coefficient C will be 1 or -1 [35]. It can be clearly seen from Fig.2(a) that when the driving frequency is near to their eigenfrequencies, the system achieve synchronization under $k < k_c$. In order to show this resonant synchronization effect, the Arnold tongues of synchronization area are calculated with respect to the coupling rate k and the eigenfrequency ratio ω_1/ω_2 . We can see that the critical coupling

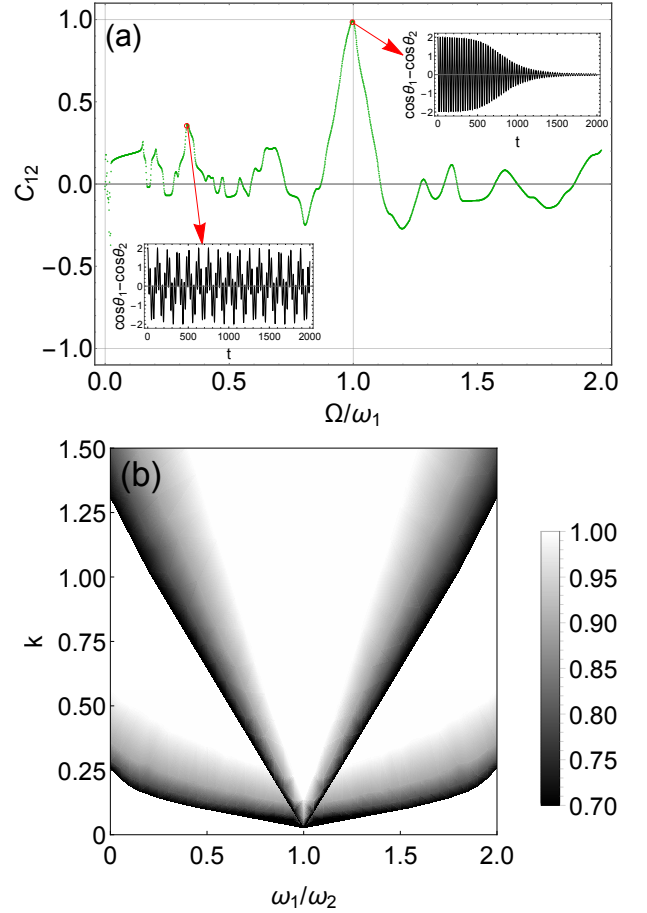


FIG. 2: (color online) (a) The synchronization degree estimated by C_{12} varies with respect to the external driving frequency Ω . The eigenfrequencies of two oscillators are $\omega_1 = 0.2, \omega_2 = 0.21$, and the coupling strength $k = 0.008$. Inset: the relative phases of two oscillators estimated by $\cos \theta_1 - \cos \theta_2$ sampled at driving frequencies of $\Omega/\omega_1 = 0.35$ and $\Omega/\omega_1 = 1$. (b) Arnold tongue describing the synchronization region estimated by C_{12} . The upper tongue area represents the synchronization without external driving, and the lower is for the case by adding the external driving with $\Lambda = 1$ and $\Omega = 0.2$.

k_c for resonant synchronization is clearly reduced and the area of synchronous region is significantly increased by the resonant driving.

C. Resonant synchronization and synchronized groups selected by resonant driving

Now, we applied the above resonant synchronization behavior to the information retrieve from our brain. The nervous system of our human brain is composed of nearly 86 billion of mutually coupled neurons [37], where dendrites or axons of neurons connect with each other through synapses to form a high-degree connected neural network [36]. By passing electrochemical signals through synapses between neurons, the neurons can be excited

or inhibited which makes the discharge of neurons in the nervous system is exactly a discontinuous non-linear process [38]. The human brain is a very complicated system [39], and thus it is impossible to reveal its functionality by just resolving the molecular structure and the function of individual neurons, but should include the discharge dynamics of the whole network formed by the individual neurons. Meanwhile, the importance of the complex network have been widely recognized in biology [41], sociology [42] as well as in physics [40], and which has been used to describe a large number of biological systems exhibiting a variety of synchronization behaviors [43]. As the complex network firstly includes a topological structure, different connections of nodes will lead to different collective dynamics. The simple model we used here is a global coupling Kuramoto model which can simulate the local function of a brain region by neglecting the connection details of the network because the collective behavior of a conscious process is somehow insensitive to the details in a high-degree connected neural network [11].

As the traditional Kuramoto model is very different from the environment of human brain and cannot be applied directly, we modify the Kuramoto model to describe critical dynamics of neurons by adaptive phase rotators [11]. The natural discharge frequency of a neuron can be represented by the eigenfrequency of KO and the more complex frequency and irregular coupling rate between neurons are considered by adding small harmonic modulations. When the system is under the coupling thresholds $k < k_c$ (near to the synchronized state), we study the dynamical synchronization between neurons when an external driving signal is added to the system in order to simulate the recall process of brain memory. In the brain, due to the changes of synapses or the neurotransmitter diffusion, the coupling strength between neurons will slowly change over time, and the neuron discharge frequency will change under the external stimuli. Hence, the modified Kuramoto model will be

$$\dot{\theta}_i = \omega_i(t) + \frac{1}{N} \sum k_{ij}(t) \sin(\theta_j - \theta_i), \quad (16)$$

where $\omega_i(t)$ and $k_{ij}(t)$ are the time-varying frequency of neuron i and the coupling strength between i and j neurons, respectively, which are supposed to be governed by the simple functions

$$\omega_i(t) = \omega_i + \beta_i \sin(2\pi f_i t + \varphi_i), \quad (17)$$

$$k_{ij}(t) = k_{ij} + \mu_{ij} \sin(2\pi g_{ij} t + \psi_{ij}), \quad (18)$$

where the parameters $\beta_i = 0.1\omega_i$, $\mu_{ij} = 0.1k_{ij}$, $f_i = 1$, $g_{ij} = 0.3$, $\varphi_i = \pi/2$ and $\psi_{ij} = \pi$ describe the amplitudes, frequencies and phase offsets of the time-varying natural frequency and coupling strength, respectively. In order to simulate information retrieve from the memory in a wakeful brain state that the neuron firing is continuously activated by successive stimuli, we introduce an activated driving of sinusoidal signal $\Lambda \sin(\Omega t - \theta_l)$, acting on l^{th}

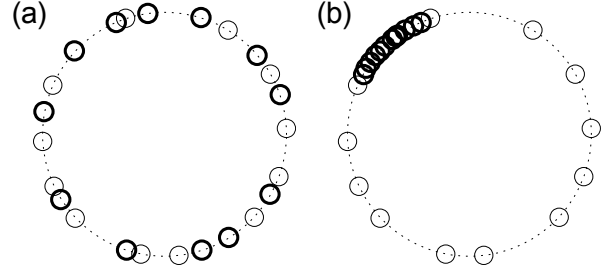


FIG. 3: Phase distributions of $N = 12$ KOs in a phase picture (a) without and (b) with the external driving after a same period of evolution. The thin circles denote the initial phase distributions of KOs and the thick ones are the phase distributions after $t = 2000$. The frequencies ω_i of the KOs are randomly sampled from the interval of $[0.9, 1.1]$ and the other parameters are $\Lambda = 1, \Omega = 1, k_{ij} = 1$.

KO (a representative oscillator selected by the stimuli in certain regions), then the equation of motion of the l^{th} oscillator becomes:

$$\dot{\theta}_l = \omega_l(t) + \frac{1}{N} \sum k_{lj}(t) \sin(\theta_j - \theta_l) + \Lambda \sin(\Omega t - \theta_l),$$

where Ω is the characteristic frequency of external stimulus. Fig.3 simulates a globally coupled network with a number of $N = 25$ KOs and demonstrates a clear phase bunching after adding an external driving signal. When the driving is added to one oscillator of the network, the oscillators whose eigenfrequencies ω_i are close to the driving frequency Ω will synchronize their motions to reach a resonant synchronization state and then the phase bunching appears. The thick circles in Fig.3(b) represents a group of synchronized oscillators which form a synchronized cluster, shown in the phase picture, moving together under the resonant driving input.

In order to show the details of the resonant synchronization, we consider $N = 6$ KOs and analyze the synchronization dynamics among these coupled KOs. In this small network, we initially set the eigenfrequencies of oscillators 1, 3, 5 randomly around 1.0, and 2, 4, 6 around 2.0 with a small deviation (see the parameters in Fig.4). Here, the eigenfrequencies set in advance stand for the stored information in the neural molecular which is characterized by its firing eigenfrequency ω_i . When an external signal with a driving frequency of $\Omega_1 = 1$ is added to one KO node of the network (see the bottom left inset of Fig.4), the oscillators 1, 3 and 5 synchronize into a group with the enhanced mutual Pearson correlation coefficients shown in Fig.4 (see the resonant peaks of curves C_{13} , C_{35} and C_{15}). If the driving frequency of $\Omega_2 = 2$ is added (see the bottom right inset of Fig.4), the KOs of 2, 4 and 6 are synchronized group instead (see the resonant peaks of curves C_{24} , C_{46} and C_{26}) due to the resonant synchronization selected by the external stimuli with different resonant frequencies.

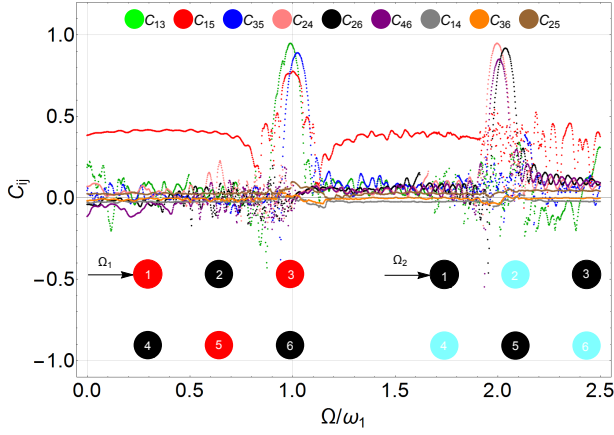


FIG. 4: (color online) The resonant synchronization of $N = 6$ KOs estimated by C_{ij} versus the driving frequency Ω . The eigenfrequencies of the oscillators are $\omega_1 = 0.94$, $\omega_3 = 1$, $\omega_5 = 1.06$, $\omega_2 = 1.97$, $\omega_4 = 2$, $\omega_6 = 2.03$, respectively, and the coupling strength and the driving strength $k_{ij} = 0.36$, $\Lambda = 1$. Two different driving frequencies are $\Omega_1 = 1$ and $\Omega_2 = 2$. Insets: the networks of 6 KOs driven by external signals with frequencies of Ω_1 (left) and Ω_2 (right), different colors stand for different synchronization groups.

D. The pattern retrieved from the memorized lattice network by resonant synchronization

Now, we will show how to recover a stored image in our brain by using well-connected network of KOs based on the resonant synchronization. As we know, the information in our brain, no matter stored or retrieved, are all activated by receiving signals inside or outside our mind. Therefore, the memory is established by the dynamic responses of neurons to different input stimuli. The different stimuli will construct different neuron molecules whose properties are characterized by different dynamic responses such as the firing eigenfrequencies we choose here in our present model. In order to reveal this, we investigate the synchronized behaviors of neurons in a regular neural network induced by the external driving sources based on the above modified Kuramoto model. We use a globally coupled neural network of 20×20 KO lattice to simulate the well-connected neurons in a local area of cerebral cortex in our brain. Here, we use frequency to code the information in the neural network. The eigenfrequency values of the coded KOs are set in advance by a Gaussian distribution with the same mean value to construct an image of “5” through a spatial configuration in the lattice network, and the eigenfrequencies of the other KOs are assigned randomly (no code area). If the lattice network is subjected to an external stimulus with a resonant driving frequency, the neurons with closed eigenfrequencies are activated and then synchronized together by the resonant driving. All the KOs with enhanced C_{ij} recover a synchronized pattern of “5” emerging in the brain. The robust effect of resonant

synchronization to retrieve the pattern “5” is shown in Fig. 5. The images in the left column, Fig. 5(a)(c), are displayed by the mutual synchronous matrix of C_{ij} without adding stimulus signals, while the images in the right column, Fig. 5(b)(d), are C_{ij} with stimulus of $\Omega = 1$. When we add the driving signal to the network, the resonant synchronization pattern appears that the synchronized KOs with similar stored eigenfrequencies are activated and connected with each other by the driving stimulus (right column). If there is no input, all KOs are oscillating at their own eigenfrequencies independently, and the dynamics of the whole network is indeed random and no regular pattern is produced (left column). Therefore, by a direct simulation, we can find a clear pattern emergence of a stored image if an external stimulus is added.

Considering that the human memory is a complex network with a large number of randomly arranged neurons immersed in a noisy background, the dynamics of neurons in the human brain may not as simple as that we considered above, but this simple model can hold the main idea of the searching mechanism of our memory. When

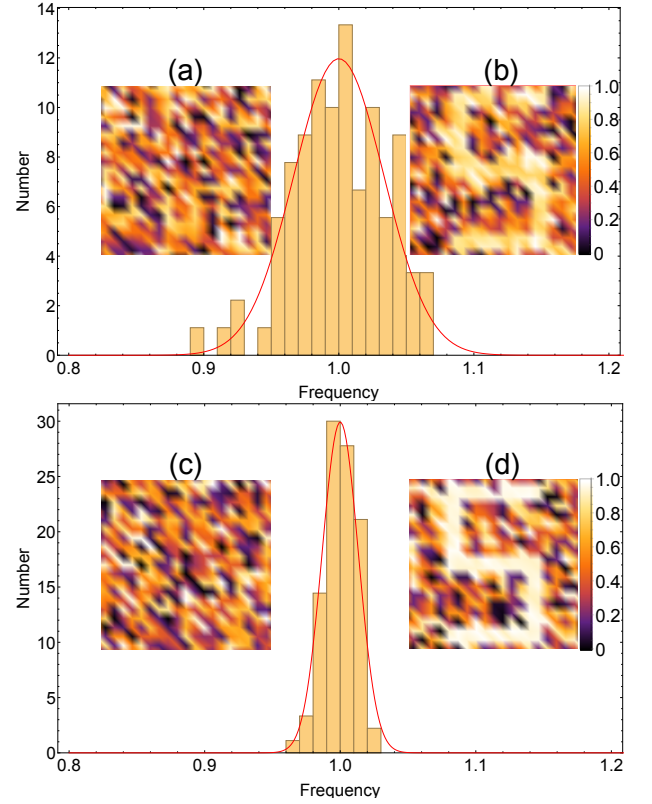


FIG. 5: (color online). Memory synchronization pattern retrieved from C_{ij} with resonant driving (b)(d) and without external driving (a)(c). The frequencies of the memorized oscillators are assigned by Gaussian distributions with mean value of 1 and the deviations 0.1/3 (the upper one) and 0.04/3 (the lower one), the frequencies of the other oscillators are set randomly from the interval $[0, 2]$. The other parameters are $\Lambda = 1$, $k_{ij} = 0.36$.

we set the coded KOs' eigenfrequencies with Gaussian distributions of different deviations in order to consider different intensities of unavoidable noises in the memory, the resonant synchronous pattern of C_{ij} can be recovered in different resolutions. A larger deviation will lead to a more fuzzy picture of synchronized pattern as in Fig.5(b) than that of a small deviation one shown in Fig.5(d). This phenomenon is very similar to the memory of our human brain that a larger disturbance will decrease the accuracy of memory and fails an effective information extraction. Therefore, the memory needs to be repeated by decreasing the deviation of the information stored in the neuron molecules. Furthermore, if the neural network is stimulated by different types of stimulus, different synchronized patterns corresponding to different frequencies of stimuli will also be retrieved. Different information can be stored in the neurons characterized by different frequency channels and the storage capacity of information in a network is determined by the frequency discrimination of the network. If the stimuli are similar, similar mixing patterns will be retrieved from our memory, which is another important characteristic of the neural network to enable imaginations of our brain.

III. CONCLUSION

In this article, we found a robust cooperative behavior of a globally coupled network, the resonant synchronization, emerged from the modified Kuramoto oscillators, and can be used to decipher the mechanism of memory searching in the human brain. Physically, the stimuli from our sensory organs will construct neural networks in our brain with different characteristics of neurons (derived from different molecular components),

whose reactive properties here are denoted by their responsive frequencies of electrical pulsing. Different frequencies denote different kind of information stored in the neural network. We simulate the collective responses of the well-connected network to the external stimuli, and the resonant synchronized pattern of the KOs with similar eigenfrequencies appears in a regular KOs network. The results show that there exists a significant enhancement of collective dynamics with the synchronized motions induced by external driving and which exhibits dramatically different behaviors from that without driving. Under the influence of input driving on a critical network, all the oscillators (nodes) whose frequencies are close to the frequency of external driving are activated and synchronized, just like the recall process in our memory to get all the resonant (similar) information by certain stimulus. There are many different types of memories in our brain, the light, the sound or the pressure, etc., they all can be selected and extracted by different types of electric stimuli from our different sensory organs, and the irrelevant information will be suppressed and can not be activated by resonant effect. The resonant synchronization to retrieve information from our brain is a quick, efficient and robust information searching way and, basically, it is also a simple and universal phenomenon in physics.

Acknowledgments

This work was supported by the National Natural Science Foundation of China (Grant No. 11447025) and the Scientific Research Foundation for Returned Overseas Chinese Scholars of the State Education Ministry.

-
- [1] F. P. Battaglia, and A. Treves, *Attractor neural networks storing multiple space representations: A model for hippocampal place fields*, *Phys.Rev.E* **58**, 7738–7753 (1998).
 - [2] E.R. Colman, and D.V. Greetham, *Memory and burstiness in dynamic networks*, *Phys.Rev.E* **92**, 012817 (2015).
 - [3] V.V. Kapelko, and A.D. Linkevich, *Chaos and associative generation of information by networks of neuronal oscillators*, *Phys.Rev.E* **54**, 2802–2806 (1996).
 - [4] J. C. Comte, and P. Ravassard, and P.A. Salin, *Sleep dynamics: A self-organized critical system*, *Phys.Rev.E* **73**, 056127 (2006).
 - [5] M. V. L. Bennett and R.S. Zukin, *Electrical Coupling and Neuronal Synchronization in the Mammalian Brain*, *Neuron* **41**, 495–511 (2004).
 - [6] Y-y Li, G. Schmid, P. Hanggi, and L. Schimansky-Geier, *Spontaneous spiking in an autaptic Hodgkin-Huxley setup*, *Phys.Rev.E* **82**, 061907 (2010).
 - [7] E. Rossoni, Y-h Chen, M-z Ding and J-f Feng, *Stability of synchronous oscillations in a system of Hodgkin-Huxley neurons with delayed diffusive and pulsed coupling*, *Phys.Rev.E* **71**, 061904 (2005).
 - [8] P.A. Tass, T. Fieseler, J. Dammers, K.Dolan, P. Morosan, M. Maitanik, F. Bösers, A. Muren, K. Zilles, and G.R. Fink *Synchronization Tomography: A Method for Three-Dimensional Localization of Phase Synchronized Neuronal Populations in the Human Brain using Magnetoencephalography*, *Phys.Rev.Lett.* **90**, 088101 (2003).
 - [9] S.H. Strogatz, *From Kuramoto to Crawford: exploring the onset of synchronization in populations of coupled oscillators*, *Physica D: Nonlinear Phenomena* **143**, 1–20 (2000).
 - [10] Y. Kuramoto, *Chemical Oscillations, Waves, and Turbulence*, *Springer-Verlag Berlin Heidelberg* **19**, VIII, 158 (1984).
 - [11] D. Cumin and C. Unsworth, *Generalising the Kuramoto model for the study of neuronal synchronisation in the brain*, *Physica D:Nonlin. Phenom.* **226**,181–196 (2007).
 - [12] T.Y. Kori, M. Naoki, *Self-organization of feed-forward structure and entrainment in excitatory neural networks with spike-timing-dependent plasticity*, *Phys.Rev.E* **79**, 051904 (2009).
 - [13] A. Nordenfelt, J. Used, and M.A.F. Sanjuán, *Bursting*

- frequency versus phase synchronization in time-delayed neuron networks, *Phys.Rev.E* **87**, 052903(2013).
- [14] S. Mofakham, C.G. fink, V. Booth, and M.R.Zochowski, *Interplay between excitability type and distributions of neuronal connectivity determines neuronal network synchronization*, *Phys.Rev.E* **94**, 042427 (2016).
- [15] C.A.S. Batista, E.L. Lameu, A.M. Batista, S.R. Lopes, T. pereira, G. Zamora-López, J.Kuths, and R.L. Viana, *Phase synchronization of bursting neurons in clustered small-world networks*, *Phys.Rev.E* **86**, 016211 (2012).
- [16] A. Szorkovszky, A. C. Doherty, G. I. Harris, and W. P. Bowen, *Mechanical Squeezing via Parametric Amplification and Weak Measurement*, *Phys.Rev.Lett.* **107**, 213603 (2011).
- [17] K.L. Snyder, and C.T. Farley, *Energetically optimal stride frequency in running:the effects of incline and decline*, *J.Exp.Biol.* **214**, 2089-2095 (2011).
- [18] S. Perisanu, T. Barois, A. Ayari, P. Poncharal, M. Choueib, S.T. Purcell, and P. Vincent, *Beyond the linear and Duffing regimes in nanomechanics: Circularly polarized mechanical resonances of nanocantilevers*, *Phys.Rev.B* **81**, 165440 (2010).
- [19] J.A. Sidles, and D. Rugar, *Signal-to-noise ratios in inductive and mechanical detection of magnetic resonance*, *phys.Rev.Lett.* **70**, 3506-3509 (1993).
- [20] X. Jiang, Y. Li, B.Liang, J.C. Cheng, and L. Zhang, *Convert Acoustic Resonances to Orbital Angular Momentum*, *Phys.Rev.Lett* **117**, 034301 (2016).
- [21] G.S. Wiederhecker, A. Brenn, H.L. Fragnito, and P.St.J. Russell, *Coherent Control of Ultrahigh-Frequency Acoustic Resonances in Photonic Crystal Fibers*, *Phys.Rev.Lett.* **100**, 203903 (2008).
- [22] A. Pikovsky, M. Rosenblum, J. Kurths, *Synchronization A Universal Concept in Nonlinear Sciences*, *Cambridge Nonlinear Science Series.* (2003).
- [23] E. Amitai, N. Lörch ,A. NunnenkamP, S. Walter, And C. Bruder, Christoph, *Synchronization of an optomechanical system to an external drive*, *Phys.Rev.A* **95**, 053858 (2017).
- [24] H. Sompolinsky, D. Golomb, and D. Kleinfeld, *Cooperative dynamics in visual processing*, *Phys.Rev.A* **43**, 6990-7011 (1991).
- [25] M. Cassidy, P. Mazzone, A. Oliviero, A.Insola, P. Tonali, V.D. Lazzaro, P. Brown, *Movement-related changes in synchronization in the human basal ganglia*, *Brain.* **125**, 1235-1246 (2002).
- [26] W. Klimesch, *Memory processes, brain oscillations and EEG synchronization*, *Int.J.Prost.* (1996).
- [27] D. Abásolo , R. Hornero , C. Gómez , M. García and M. López, *Analysis of EEG background activity in Alzheimer's disease patients with Lempel-Ziv complexity and central tendency measure*, *Med.Eng.Phys.* **28**, 315 - 322 (2006).
- [28] F. Mormann , K. Lehnertz and P. David and C. E. Elger, *Mean phase coherence as a measure for phase synchronization and its application to the EEG of epilepsy patients*, *Physica D: Nonlinear Phenomena.* **144**, 358 - 369 (2000).
- [29] P. Bethany and D. Rhonda and Z. Michal and P. Jack, *Transition from local to global phase synchrony in small world neural network and its possible implications for epilepsy*, *Phy. Rev. E* **72**, 031909 (2005).
- [30] F. Mormann, R.G. Andrzejak, T. Kreuz, C. Rieke, P. David, C.E. Elger, and K. Lehnertz , *Automated detection of a preseizure state based on a decrease in synchronization in intracranial electroencephalogram recordings from epilepsy patients*, *Phys.Rev.E* **67**, 021912 (2003).
- [31] Y-C Lai, M.G. Frei, I. Osorio, and L. Huang, *Characterization of Synchrony with Applications to Epileptic Brain Signals*, *Phys.Rev.Lett* **98**, 108102 (2007).
- [32] S.C. O'Connor and P.A. Robinson, *Spatially uniform and nonuniform analyses of electroencephalographic dynamics, with application to the topography of the alpha rhythm*, *Phys.Rev.E* **70**, 011911 (2004).
- [33] M.P.K. Jampa, A.R. Sonawane, P.M. Gade, and S.Sinha, *Synchronization in a network of model neurons*, *Phys.Rev.E.* **75**, 026215 (2007).
- [34] D.H. Zanette, *Disturbing synchronization: Propagation of perturbations in networks of coupled oscillators*, *Eur. Phys. J. B* **43**, 97-108 (2005).
- [35] L. Maccone, D. Bruß, and C. Macchiavello, *Complementarity and Correlations*, *Phys.Rev.Lett.* **114**, 130401 (2015).
- [36] S.J. Wang, X.J. Xu, Z.X. Wu. and Y.H. Wang, *Effects of degree distribution in mutual synchronization of neural networks*, *Phys.Rev.E* **74**, 041915 (2006).
- [37] S.Herculano-Houzel, *The human brain in numbers: a linearly scaled-up primate brain*, *Human neuroscience* **3**, 31 (2009).
- [38] A.L. Hodgkin, A.F. Huxley, *A quantitative description of membrane current and its application to conduction and excitation in nerve*, *J.Physiol.* **117**, 1469-7793 (1952).
- [39] V.A. Maksimenko, A.E. Runnova, N.S. Frolov, V.V. Makarov, V. Nedaivozov, A.A. Koronovskii, A. Pisarchik, and A.E. Hramov, *Multiscale neural connectivity during human sensory processing in the brain*, *Phys.Rev.E* **97**, 052405 (2018).
- [40] D. Cimpoesu, A. Stancu, and L. Spinu, *Physics of complex transverse susceptibility of magnetic particulate systems*, *Phys.Rev.B.* **76**, 054409 (2007).
- [41] A.V. Goltsev, F.V. de Abreu , S.N. Dorogovtsev, and J.F.F Mendes, *Stochastic cellular automata model of neural networks*, *Phys.Rev.E* **81**, 061921 (2010).
- [42] L. de Sanctis, and T. Galla, *Effects of noise and confidence thresholds in nominal and metric Axelrod dynamics of social influence*, *Phys.Rev.E* **79**, 046108 (2009).
- [43] A. Venaille, P. Varona, M.J. Rabinovich, *Synchronization and coordination of sequences in two neural ensembles*, *Phys.Rev.E* **71**, 061909 (2005).